


ORIGINAL ARTICLE

Open Access



The role of MRI-R2* in the detection of subclinical pancreatic iron loading among transfusion-dependent sickle cell disease patients and correlation with hepatic and cardiac iron loading

Basant Mohamed Raief Mosaad^{1*} , Ahmed Samir Ibrahim¹, Mohamed G. Mansour¹, Mohsen Saleh ElAlfy², Fatma Soliman Elsayed Ebeid² and Emad H. Abdeldayem¹

Abstract

Objectives: Pancreatic reserve could be preserved by early assessment of pancreatic iron overload among transfusion-dependent sickle cell disease (SCD) patients. This study aimed to measure pancreatic iron load and correlate its value with patients' laboratory and radiological markers of iron overload.

Materials and methods: Sixty-six SCD children and young adults underwent MRI T2* relaxometry using a simple mathematical spreadsheet and laboratory assessment.

Results: The results indicated moderate-to-severe hepatic iron overload among 65.2% of studied cases. None had cardiac iron overload. Normal-to-mild iron overload was present in the pancreas in 86% of cases, and 50% had elevated serum ferritin > 2500 ug/L. There was no significant correlation between pancreatic R2* level, serum ferritin, and hepatic iron overload. Patients with higher levels of hemolysis markers and lower pre-transfusion hemoglobin levels showed moderate-to-severe pancreatic iron overload.

Conclusion: Chronically transfused patients with SCD have a high frequency of iron overload complications including pancreatic iron deposition, thereby necessitating proper monitoring of the body's overall iron balance as well as detection of extrahepatic iron depositions.

Keywords: Pancreatic R2*, Sickle cell disease, MRI T2*

Key points

- Transfusion-dependent SCD patients did not demonstrate cardiac siderosis.
- A total of 86% of transfusion-dependent SCD patients had normal-to-mild pancreatic iron overload.
- No correlations were found between pancreatic R2* level, transfused iron, or hepatic iron.

*Correspondence: basantraief@gmail.com

¹ Radiology Department, Faculty of Medicine, Ain Shams University, Cairo, Egypt

Full list of author information is available at the end of the article

Introduction

Sickle cell disease (SCD) is an autosomal recessive hematological disorder involving production of abnormal sickle hemoglobin (HbS) [1]. The responsible gene exists in the Egyptian western desert near the Libyan border with variable rates of 0.38% in coastal areas and up to 9.0% in the new valley oases, mostly of the African globin gene haplotype [2].

Although wider use of hydroxycarbamide and new therapeutic approaches have improved health-related quality of life, SCD in lower-resource countries still carries a poor prognosis and is associated with high early childhood mortality [3]. Transfusion is a frequently employed therapy that is best validated for prophylaxis and treatment of acute chest syndrome (ACS) [4]; about 90% of adult patients have received a transfusion at least once in their lifetimes [3]. Although transfusion improves disease severity and complications, severe iron overload is an inevitable complication, and chronically transfused iron-overloaded SCD patients have higher mortality than those with fewer transfusions and without iron overload [5].

Magnetic resonance imaging (MRI) is noninvasive, inexpensive, and widely available in developed countries [6]. Although serum ferritin is clinically used to estimate body iron stores, it reflects only around 1% of the total iron storage pool, and its measurement can be confounded by many conditions. In addition, liver iron content measured through MRI, which serves as a better indicator of whole-body iron, does not reflect heart iron loading [7]. The pancreatic iron burden may precede cardiac iron loading and is a powerful predictor of heart iron overload, and its early assessment and tailored chelation could prevent diabetes and preserve pancreatic reserve [8].

The primary purpose of this work was to quantitatively assess pancreatic iron loading in transfusion-dependent SCD patients. The secondary purposes were to assess pancreatic iron load in correlation to hepatic and cardiac iron load using MRI and to delineate the relationship between pancreatic iron load, clinical outcomes, and laboratory tests including serum ferritin and amylase.

Materials and methods

Patient population

This cross-sectional study included 66 children and young adults with SCD who were recruited as regular patients of the Pediatric Hematology Clinic, Children's Hospital, a tertiary university hospital. Participation in the study was voluntary and required informed consent from the patients and/or their legal guardians. The study was approved by the institutional regulatory board of the

Pediatric University Hospital. All procedures adhered to the ethical standards of the responsible committee on human experimentation (institutional and national) and with the Helsinki Declaration of 1975, as revised in 2008.

Inclusion criteria

- Older than 5 years and able to perform MRI study.
- Patients with SCD who received packed RBCS blood transfusion more than 20 times in their lives showed an increased risk of iron overload. Thus, chelation therapy should be considered (according to National Cancer Comprehensive Network Clinical Practice Guidelines in Oncology [9]).

Exclusion criteria

- Known to have contraindications for MRI, such as an implanted magnetic device, pacemaker, or claustrophobia.
- History of myocardial infarction, cardiac failure, or hepatic failure.
- Affliction with other transfusion-dependent diseases.

All recruited patients were subjected to detailed medical history review and full clinical examination with special emphasis on disease duration, anthropometric measures, cardiac disease, history of splenectomy, viral hepatic infection, and history of transfusion or chelation therapy. The transfusion that was received was calculated as transfusion index: volume of transfused packed red cells in ml per kg body weight per year.

Patients with SCD received monotherapy or combined chelation therapy. Mono-chelation included deferoxamine (DFO) infused subcutaneously in a dose that ranged from 30 to 45 mg/kg/day given 5 days/week, oral deferoxamine (DFP) in a daily dose ranging from 50 to 100 mg/kg/day, or oral deferasirox (DFX) in a daily dose of 40 mg/kg/day. Assessment of patients' compliance with chelation therapy involved reviewing patient self-reports, and the number of doses taken each day was checked using prescription refills and pill counts. A cutoff point below 80% was considered poor compliance to the regimen [10]. Hydroxyurea therapy was given orally in a dose of 20 mg/kg/day, with an increase to the maximum tolerated dose according to safety and response.

Laboratory analysis

Peripheral venous blood samples were collected on potassium-ethylenediaminetetraacetic acid (K2-EDTA) for complete blood count (CBC) using Sysmex

XT-1800i (Sysmex, Kobe, Japan) hemoglobin analysis by HPLC using D-10 (BioRad, Marnes La Coquette, France). To perform the chemical analysis and enzyme-linked immunosorbent assay (ELISA), clotted samples were obtained, and serum was separated by centrifugation for 15 min to perform liver function tests (including serum albumin, total bilirubin, alanine aminotransferase, aspartate aminotransferase, lactate dehydrogenase, and indirect bilirubin) using Cobas Integra 800 (Roche Diagnostics, Mannheim, Germany). Serum ferritin level was measured using the Immulite 1000 analyzer (Siemens Healthcare Diagnostics, Marburg, Germany) and accompanied by the calculation of the patient's mean value of the year before the study to assess ferritin trend. As per relevant literature, the cut-off value of 2500 $\mu\text{g/L}$ was used to classify patients into two groups as this has been defined as the best predictor of thalassemia complication [11].

Magnetic resonance imaging (MRI) acquisition and image analysis

MRI examination was performed on a 1.5 Tesla superconductive MR Philips scanner (Achieva; Philips Medical Systems, Best, The Netherlands) in a tertiary university hospital without any contrast material. Patients were prepared and informed to remain motionless, avoid excessive swallowing, adjust respiration, and avoid several diaphragmatic motions. The duration of the study took approximately 10–15 min, and the system produced some loud noises.

(A) To complete quantitative measurement of pancreatic iron loading ($R2^*$), the following steps were taken.

- Upper abdominal axial cuts were taken using a multi-echo gradient sequence at 12 simultaneous echo times (TE) with a field-of-view (FOV) span from the dome of the diaphragm to the inferior poles of the kidneys to ensure complete pancreatic coverage by 25 slices.
- The region of interest (ROI) was manually drawn over the pancreatic head or tail encompassing parenchymal tissue (mostly drawn over the pancreatic head) and took care to avoid confounding anatomy (large blood vessels or ducts) and areas with susceptibility artifacts from gastric or colic intraluminal gas. Then, the ROI was copied across all images.
- Grading of pancreatic iron loading ($R2^*$): Normal: < 30 Hz, Mild: 30–100 Hz, Moderate: 100–400 Hz, and Severe: > 400 Hz [12].

(B) To complete quantitative measurement of myocardial $T2^*$, the following steps were taken:

- Multi-echo turbo field echo (mTFE) cardiac black and white blood short-axis were obtained using ECG and respiratory-gated with a dedicated 12-element phased-array Torso coil using single 8–12 s breaths.
- The ROI was drawn in the interventricular septum encompassing both endocardial and epicardial regions.
- Grading of cardiac iron loading $T2^*$: Normal > 20 ms, Mild: 15–20 ms, Moderate: 10–15 ms, and Severe < 10 ms [13].

(C) To quantitatively measure liver iron concentration (LIC), the following steps were taken:

- Upper abdominal axial cuts were taken using a multi-echo gradient sequence where the signal intensity of the liver parenchyma was acquired using region-based measurement.
- The ROI was placed over an axial mid-hepatic slice of the right hepatic lobe in an area free from vessels and bile ducts.
- Liver siderosis was measured using relaxation parameter $T2^*$, and liver $T2^*$ values were then converted into $R2^*$ values ($= 1000/T2^*$). Finally, LIC (mg/gdw) were calculated according to Garbowski et al.'s equation: $LIC = 0.03 \times R2^* + 0.7$ [14].
- Grading of liver iron loading LIC: Normal < 2 mg/g, Mild: 2–7 mg/g, Moderate: 7–15 mg/g, and Severe > 15 mg/g [15].

The pancreatic R^* as well as myocardial and liver $T2^*$ were manually calculated via simple mathematical models by using Microsoft Excel Spread Sheet V3.0 [16]. The mean value of the signal intensity along different TE values was manually input into an Excel spreadsheet, and then, a curve-fitting truncation model consisting of a mono-exponential decay curve was applied [17].

(D) To qualitatively assess the renal iron overload:

- The upper abdominal axial cuts that were taken for coverage of the whole pancreatic tissue by 25 slices with a FOV spanning from the dome of the diaphragm to the inferior poles of the kidneys were used for qualitative assessment of the renal iron overload.
- The renal cortices contained the highest concentrations of glomeruli and proximal tubules, and the micro-anatomic locations contained the greatest iron deposition. Excess renal iron overload was determined by the presence of a hypointense signal of the renal cortex compared to the medulla on the T1-weighted images and accentuated reduction in cortical signal intensity on the T2-weighted images.

Statistical analysis

The data were analyzed using Stata[®] version 14.2 (Stata-Corp LLC, College Station, TX, USA) and MedCalc[®] version 15.8 (MedCalc[®] Software bvba, Ostend, Belgium). Quantitative variables were described in the form of mean and standard deviation or median and interquartile range (IQR; 75th and 25th percentiles). Qualitative variables were described as numbers and percentages. The Kolmogorov–Smirnov test was used to test the distribution of normality. To compare parametric quantitative variables between two groups, Student's *t* test was applied. To compare nonparametric quantitative variables between two groups, the Mann–Whitney test was used. Qualitative variables were compared using the chi-square (χ^2) test or Fischer's exact test when frequencies were below five. Pearson correlation coefficients were used to assess the association between two normally distributed variables. When a variable was not normally distributed, a Spearman correlation test was performed. A *p* value < 0.05 was considered significant in all analyses.

Results

This study included 66 patients ($n = 66$; 31 females and 35 males; 15.68 ± 7.02 years of age) with a history of SCD who had received repeated blood transfusions for cardiopulmonary complications and ACS (33.3%, 22 patients) as a secondary stroke preventive measure (13.7%, 9 patients) and for frequent sickling crisis and symptomatic anemia (53.0%, 35 patients).

Among the 66 patients, only 53 received chelation therapy. Of these 53 patients, 92.5% (49 patients) received monotherapy as follows: 35 patients (71.4%) received DFP, 13 patients (26.5%) received DFO, and only one patient (2.1%) received DFX. The remaining four patients (7.5%) required combined chelation therapy for the treatment of iron overload. Demographic, clinical, laboratory, and radiological characteristics of the studied patients with SCD are illustrated in Table 1.

Most of the patients (65.2%, 43 patients) demonstrated moderate-to-severe hepatic iron overload, 13.6% (9 patients) demonstrated moderate-to-severe iron overload within the pancreatic tissue, and none had a cardiac iron overload. Twenty-eight patients revealed a marked decrease in renal cortical signal intensity with almost sparing of the renal medulla (Figs. 1, 2).

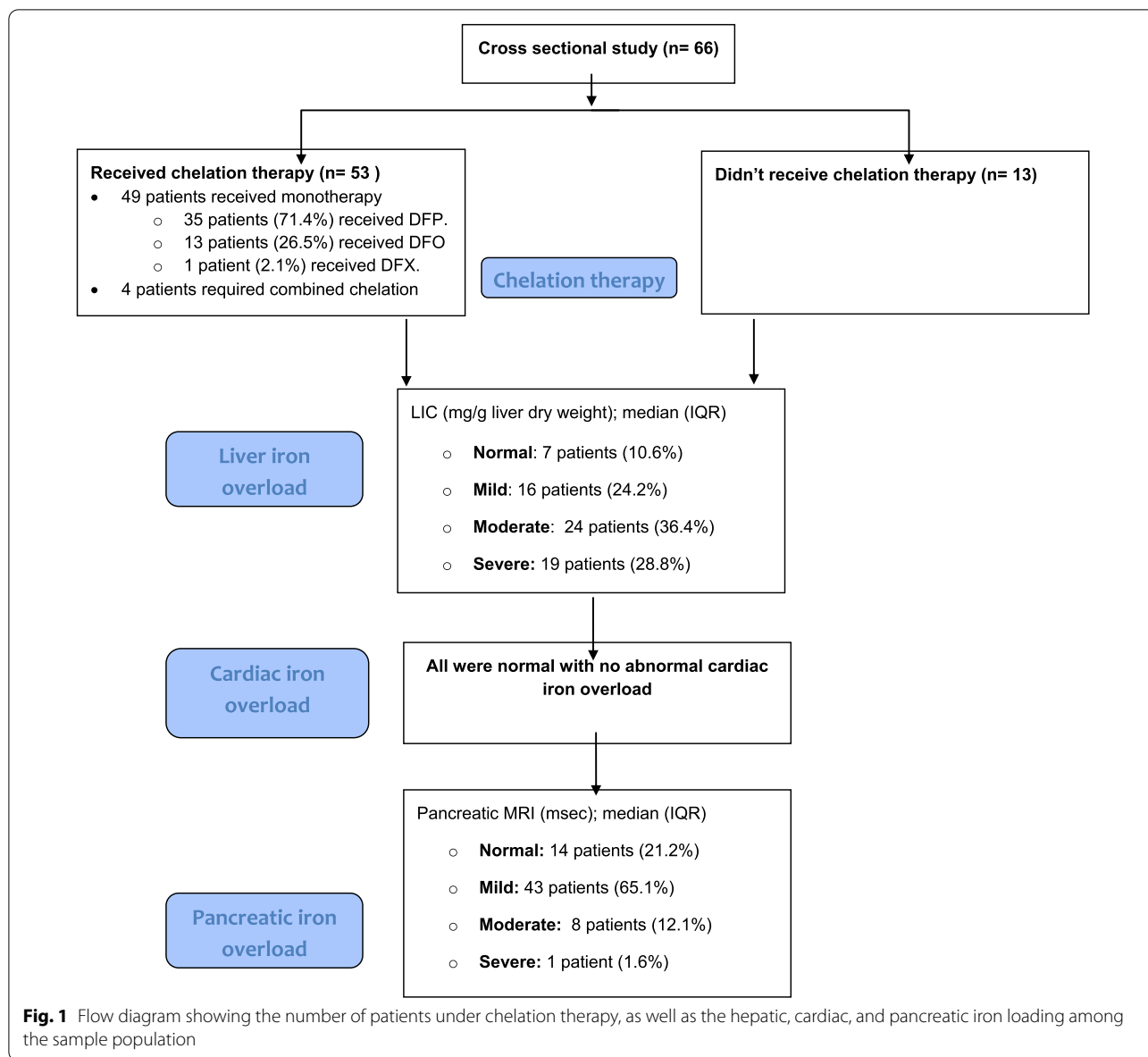
To study the possible correlation between pancreatic iron overload in SCD patients, a comparison between SCD patients with normal pancreatic MRI and those with moderate-to-severe pancreatic MRI was performed, as illustrated in Table 2. The mild subgroup was omitted from this comparative study for two reasons. Firstly, the mild subgroup had a narrow zone of Hz of only 0–100

Table 1 Characteristics of the studied patients with sickle cell disease

Variable	Sickle cell disease ($n = 66$)
Age (year); mean \pm SD	15.68 \pm 7.02
Male: female, n (%)	35 (53.0%): 31 (47.0%)
Positive family history of SCD, n (%)	43 (65.2%)
<i>Clinical characteristics</i>	
Splenectomized, n (%)	13 (20.0%)
Number of sickle crisis/year; median (IQR)	4 (2–8)
Sickle crisis \geq 3/year, n (%)	35 (54.7%)
History of silent or manifest stroke, n (%)	9 (14.1%)
History of acute chest syndrome, n (%)	12 (18.8%)
Cardiopulmonary complications, n (%)	10 (15.6%)
Transfusion index (mL/kg/year)	120 (60–240)
Iron overload per day (mg/kg); mean \pm SD	0.23 \pm 0.15
On chelation therapy, n (%)	53 (80.3%)
Poor compliance to chelation, n (%)	21 (42.0%)
<i>Laboratory characteristics</i>	
Pre-transfusion hemoglobin (g/dL); mean \pm SD	8.03 \pm 1.42
HbS (%); mean \pm SD	61.33 \pm 20.70
HbF (%); median (IQR)	4.7 (1.3–12.2)
Serum amylase (U/L); mean \pm SD	56.73 \pm 21.43
Serum ferritin (μ g/L); median (IQR)	2805 (median 940–4638)
Serum ferritin level > 2500; n (%)	33 (50%)
<i>Radiological characteristics</i>	
LIC (mg/g liver dry weight); median (IQR)	11.63 (5.81–20.31)
Normal; n (%)	7 (10.6%)
Mild; n (%)	16 (24.2%)
Moderate; n (%)	24 (36.4%)
Severe; n (%)	19 (28.8%)
Cardiac T2* (msec); mean \pm SD	31.40 \pm 6.58
Normal; n (%)	66 (100%)
Pancreatic MRI (msec); median (IQR)	53.80 (35.35–84.45)
Normal; n (%)	14 (21.2%)
Mild; n (%)	43 (65.1%)
Moderate; n (%)	8 (12.1%)
Severe; n (%)	1 (1.6%)

versus the moderate (100–400) and severe zones (more than 400 Hz). Secondly, the mild subgroup was in the gray zone between normal and significant iron overloading. Thus, adding this group with a relatively high percentage ratio (65.1%) of abnormal pancreatic MRI to the sample would have produced a great impact on the results.

Patients who presented with a high level of hemolysis marker and a low level of pre-transfusion hemoglobin exhibited moderate-to-severe pancreatic MRI iron overload. Although the percentage of non-compliance to chelation therapy was higher (71.4%) in those who



had abnormal pancreatic MRI than those with normal MRI (45.5%), the difference does not have statistical significance. To highlight the effect of iron overload, a comparison between SCD patients who had serum ferritin less than or equal to 2500 ug/L and those with high serum ferritin of more than 2500 ug/L was also performed, as illustrated in Table 3.

A correlation study of pancreatic MRI among the SCD patients revealed that there was a non-significant negative correlation between pancreatic MRI and transfusion index ($p=0.314$), iron overload per day ($p=0.424$), pre-transfusion hemoglobin ($p=0.051$), serum amylase ($p=0.730$), HbS% ($p=0.663$), and serum ferritin ($p=0.964$). In addition, there was a non-significant

positive correlation with LIC ($p=0.069$). Furthermore, there was no significant correlation between serum amylase and other studied parameters.

Discussion

Transfusion is used in patients with SCD to increase blood's oxygen-carrying capacity and to improve blood flow [4]. The recruited children and young adults with SCD were a unique population who received frequent transfusions as prophylaxis and as therapy for major complications of SCD. However, iron overload is an unavoidable complication of transfusions [4]; consequently, the studied SCD patients presented high iron overload/

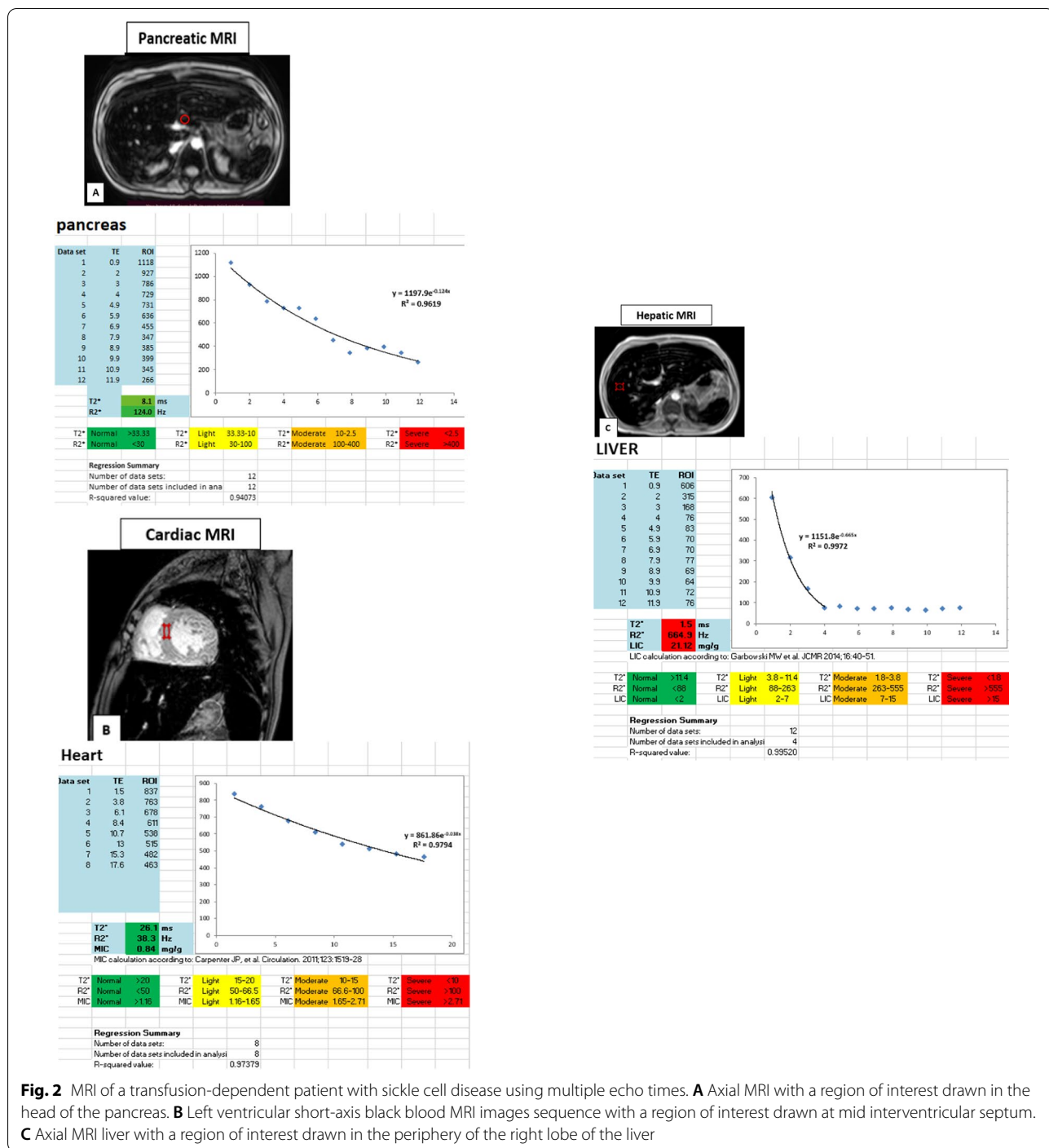


Fig. 2 MRI of a transfusion-dependent patient with sickle cell disease using multiple echo times. **A** Axial MRI with a region of interest drawn in the head of the pancreas. **B** Left ventricular short-axis black blood MRI images sequence with a region of interest drawn at mid interventricular septum. **C** Axial MRI liver with a region of interest drawn in the periphery of the right lobe of the liver

day with an estimated average value of 0.23 ± 0.15 mg/kg, which leads to iron accumulation. Fortunately, 80.3% of the studied patients received monotherapy chelation.

MRI does not image iron directly; it images water protons diffusing near iron deposits [6], which causes local distortion in the magnetic field inhomogeneity ($T2^*$) and

loss of signal intensity in proportion to its deposition [18]. MRI represents a safe, noninvasive, highly reproducible modality [19, 20] that provides new insights into the dynamics of iron overload [21].

Iron causes MRI images to darken at a rate proportional to the hepatic iron load, with the half-life of this

darkening defined as $T2^*$. The rate of darkening, designated as $R2^*$, is the reciprocal of $T2^*$ and is proportional to the iron content of the tissues. MRI scanning estimates tissue iron concentration both by gradient echo imaging, which provides $T2^*$, and spin echo imaging, which provides $T2$, the reciprocal of $R2$ [22].

$R2$ and $R2^*$ methods have respective theoretical advantages and disadvantages. $R2$ techniques are insensitive to the size and shape of the imaging “voxel” as well as external magnetic inhomogeneities, while $R2^*$ methods can be influenced by these factors. In contrast, $R2^*$ measurements are more robust to variations in the length scale of iron deposition and can accurately reflect the bulk magnetic susceptibility of tissues. $R2^*$ measurements can also be performed in a single breath-hold, while $R2$ methods take 5 to 20 min (depending on technique). $R2^*$ measurements are robust to long-range magnetic disturbances; thus, one would expect a linear relationship between $R2^*$ and iron over the entire physiologic range of iron deposition [23, 24].

There are two basic types of pulse sequences: the spin echo (SE) and the gradient echo (GRE). To measure signal intensity and quantify iron concentration, GRE $T2^*$ and SE $T2$ sequences are used. The GRE sequence generates a $T2^*$ decay curve, which is much faster and very

sensitive even to small amounts of iron deposition. In contrast, the SE sequence generates a $T2$ decay curve, which is a more time-consuming process [25].

In the current study, MRI $T2^*$ relaxometry method was used to concurrently quantify hepatic, myocardial, and pancreatic iron in the same setting with short acquisition times and fast scanning through the multi-echo sequence, which is particularly beneficial in the pediatric population. A range of echo times was used to allow accurate quantification of $T2^*$ values in cases of severe iron overload and to provide suitable sensitivity at low tissue iron levels. The use of constant repetition time between all echo times eliminated any $T1$ effects that might skew the data when using the conventional sequence [26].

There is no definitive gold standard for $T2^*$ post-processing [15]. Consequently, iron content was calculated in the current study through a relatively inexpensive, commercially available Excel spreadsheet with a linear mono-exponential fitting model that is reported to have a slightly higher coefficient of variation compared with the nonlinear fitting used in CMR tools [16]. This Excel-based approach would be the most accessible program for most physicians, especially in limited-resource settings, and avoids the complicated extra technical step and costs of licensing the necessary complementary bases.

Table 2 Comparison between sickle cell disease patients with normal and those with abnormal pancreatic MRI

Variable	Normal pancreatic MRI (n = 14)	Abnormal* pancreatic MRI (n = 9)	p value
Age (years); mean \pm SD	17.79 \pm 8.80	20.11 \pm 8.80	0.543
Males; n (%)	8 (57.1)	3 (33.3)	0.265
Transfusion index (mL/kg/year); median (IQR)	240 (120–240)	120 (60–240)	0.158
Iron Overload (mg/kg/day); mean \pm SD	0.30 \pm 0.14	0.22 \pm 0.17	0.226
On chelation; n (%)	11 (78.6)	7 (77.8)	0.964
Poor compliance to chelation; n (%)	5 (45.5)	5 (71.4)	0.280
Pre-transfusion hemoglobin (g/dL); mean \pm SD	8.74 \pm 1.64	6.61 \pm 0.54	0.004
HbS (%); mean \pm SD	67.79 \pm 24.72	54.92 \pm 25.69	0.312
HbF (%); median (IQR)	0 (0–8.2)	3.45 (3.1–12.2)	0.177
Lactate dehydrogenase (IU/L); mean \pm SD	472.14 \pm 155.57	768.38 \pm 531.13	0.062
Total bilirubin (mg/dL); mean \pm SD	2.42 \pm 1.16	4.05 \pm 1.59	0.012
Indirect bilirubin (mg/dL)	1.515 (0.96–2.1)	2.04 (1.89–2.71)	0.048
Serum amylase; mean \pm SD	62.43 \pm 24.15	70.00 \pm 32.37	0.539
Serum ferritin (ug/L); median (IQR)	3670.5 (1456–4743)	1987 (1650–4313)	0.571
Serum ferritin level > 2500; n (%)	8 (57.1)	4 (44.4)	0.552
LIC (mg/g liver dry weight); median (IQR)	14.045 (7.35–20.83)	14.03 (9.2–24.89)	0.614
Normal; n (%)	1 (7.1)	0 (0.0)	0.859
Mild; n (%)	3 (21.4)	2 (22.2)	
Moderate; n (%)	5 (35.7)	3 (33.3)	
Severe; n (%)	5 (35.7)	4 (44.4)	
Cardiac $T2^*$ (msec); mean \pm SD	31.51 \pm 4.90	29.99 \pm 3.87	0.442

Patients with Abnormal pancreatic MRI include those with pancreatic MRI > 100 Hz

Table 3 Comparison between sickle cell disease patients who had serum ferritin \leq and $>$ 2500 ug/L

Variable	Serum ferritin \leq 2500 ug/L (n = 33)	Serum ferritin $>$ 2500 ug/L (n = 33)	p value
Age (years); mean \pm SD	14.78 \pm 6.85	16.55 \pm 7.18	0.315
Males; n (%)	15 (46.9)	19 (57.6)	0.388
Iron Overload (mg/kg/day); mean \pm SD	0.17 \pm 0.14	0.28 \pm 0.13	0.001
On chelation; n (%)	20 (62.5)	32 (97.0)	0.001
Poor compliance to chelation; n (%)	6 (31.6)	15 (50.0)	0.204
Pre-transfusion hemoglobin (g/dL); mean \pm SD	7.66 \pm 1.46	8.37 \pm 1.30	0.046
HbS (%); mean \pm SD	63.28 \pm 16.04	59.57 \pm 24.29	0.504
HbF (%); median (IQR)	6.2 (0.8–12.2)	3.6 (1.3–10)	0.579
Lactate dehydrogenase (IU/L); mean \pm SD	547.38 \pm 331.71	525.21 \pm 204.67	0.749
Total bilirubin (mg/dL); mean \pm SD	2.59 \pm 1.50	2.60 \pm 1.09	0.970
Indirect bilirubin (mg/dL)	1.33 (0.9–2.18)	1.8 (0.9–2.12)	0.549
Serum amylase; mean \pm SD	57.41 \pm 24.46	56.12 \pm 18.74	0.815
LIC (mg/g liver dry weight); median (IQR)	6.19 (3.06–11.02)	16.16 (12.94–24.7)	0.000
Normal; n (%)	7 (21.9)	0 (0.0)	0.000
Mild; n (%)	13 (40.6)	2 (6.1)	
Moderate; n (%)	10 (31.3)	14 (42.4)	
Severe; n (%)	2 (6.3)	17 (51.5)	
Cardiac T2* (msec); mean \pm SD	32.03 \pm 5.09	30.79 \pm 7.80	0.454
Pancreatic MRI (msec); median (IQR)	52.85 (35.35 – 83.5)	54.9 (31.8 – 87)	0.847

The liver is the dominant storage organ for excess iron acquisition and mobilization of iron in response to iron chelation [27]. An LIC of more than seven milligrams Fe/gram dry liver weight represents the best threshold for determining the presence of hepatic fibrosis [27] and vascular morbidity [28]. The majority of patients (65.2%) had moderate-to-severe liver iron overload, confirming the previously reported finding that liver toxicity in SCD occurs at similar levels to those observed in patients with thalassemia major (TM) [28–30].

The heart, in contrast to the liver, has robust mechanisms to prevent excessive transferrin-mediated uptake [27]. The studied children and young adults exhibited moderate-to-severe hepatic iron loading, with no evidence of cardiac iron loading endorsing that chronically transfused patients with SCD had a lower risk of cardiac complication in comparison with patients with TM [31]. Delayed cardiac iron uptake compared to many other extrahepatic organs including the pancreas [32] confirms that iron overload selectively targets the liver in patients with SCA, initially relatively sparing the heart [33]. However, the heart becomes vulnerable to iron loading once the “threshold” LICs are reached, and that threshold is higher in SCD [34] (15–20 mg/g dry weight) than in TM [35].

Pancreatic iron overload can impair the exocrine and endocrine functions of the pancreas [8], which, unlike the liver, may not regenerate or remodel even with the

reduction in hemosiderosis [36]. This necessitates early assessment of pancreas iron and tailored chelation that may prevent diabetes and preserve pancreatic reserve [8]. Most of the recruited chronically transfused SCD patients (86%) had normal-to-mild pancreatic iron overload, confirming that they are less likely to develop pancreatic iron overload compared to patients with TM; this is likely because iron released by transfusion and hemolysis is efficiently handled by effective erythropoiesis [37], thus keeping transferrin saturations [38] and non-transferrin-bound iron (NTBI) levels low [39]. Furthermore, SCD patients have shorter and less intense transfusion exposure [40] even when aggressive chronic transfusion therapy is used as it is often started later in life and at a lower intensity [41]. In line with these points, Noetzli et al. found that chronically transfused SCD patients are less likely to develop moderate-to-severe pancreatic iron overload even after correcting for differences in transfusion duration, transfusion intensity, and severity of iron loading [42].

SCD patients with a history of low pre-transfusion hemoglobin levels and high levels of hemolysis markers revealed moderate-to-severe pancreatic iron MRI overload, thereby supporting the hypothetical relationship between hemolysis and pancreatic iron overload. Pancreatic iron burden precedes and is a powerful predictor of heart iron overload [8] as both organs have the same L-type calcium iron channels [36]. In this study,

pancreatic R2* did not correlate with cardiac T2* as all patients had normal cardiac T2*, and it had a nonlinear relationship with LIC. This data suggests that heavy hepatic siderosis is a prerequisite for cardiac and endocrine siderosis in SCD, unlike in TM [43], and that pancreas R2* values probably represent the most viable surrogate index for extrahepatic risk [44].

The renal cortices contain the highest concentrations of glomeruli and proximal tubules, and it is the micro-anatomic locations that contain the greatest iron deposition in SCD patients [45]; this is consistent with the finding that nearly half of patients revealed a marked decrease in renal cortical signal intensity (which represents iron loading) with almost sparing of the renal medulla. In the current study, renal iron was not quantitatively assessed, and further studies are needed to assess kidney iron burden in patients with SCD.

Conclusion

Chronically transfused patients with SCD have a high frequency of iron overload complications including pancreatic iron deposition, thus necessitating proper monitoring of the overall body iron balance as well as detection of extrahepatic iron deposition.

Study limitation

Contributions from multicenter will be of additive value to better assess such important complications of extrahepatic iron deposition. ROI positioning in the pancreatic tissue is sometimes complicated due to tissue inhomogeneities and breathing artifacts. Additionally, the pancreas may be difficult to locate in older, splenectomized subjects because of glandular apoptosis, fatty replacement, and loss of normal anatomic landmarks. Moreover, the surrounding confounding anatomy (e.g., large blood vessels or ducts) and areas involved in susceptibility artifacts from gastric or colic intraluminal gas also hinder proper pancreatic assessment and may hamper the results. The effect of iron overload upon pancreatic functioning, and especially the endocrine function, needs to be evaluated to predict the risk of diabetes mellitus among transfusion-dependent SCD patients. Renal iron was not quantitatively assessed, and further studies need to be conducted to assess kidney iron burden in patients with SCD.

Abbreviations

ACS: Acute chest syndrome; ALT: Alanine aminotransferase; AST: Aspartate aminotransferase; CBC: Complete blood count; FOV: Field of view; HbS: Sickle hemoglobin; LDH: Lactate dehydrogenase; LIC: Liver iron concentration; MRI: Magnetic resonance imaging; ms: Milliseconds; mTFE: Multi-echo turbo field echo; ROI: Region of interest; SCD: Sickle cell disease; TE: Echo time; TM: Thalassemia major.

Acknowledgements

We would like to thank the pediatric department for cooperation and for much effort throughout the work-up of our patients.

Author contributions

BMRM and FSE were responsible for conception/design of the work and imaging data. BMRM, ASI, and MSE put the idea of research, editor of the manuscript, and performed the statistical analysis. EHA and FSE participated in the design of the study and data collection. MGM was responsible for the history taking and correlation of the radiological findings with the clinical data. ASA and BMRM shared in the design of the study and image interpretation. All authors read and approved the final manuscript.

Funding

Open access funding provided by The Science, Technology & Innovation Funding Authority (STDF) in cooperation with The Egyptian Knowledge Bank (EKB). All authors declare that there is no funding or any source of financial interest.

Availability of data and materials

Available on request with the corresponding author. The authors declare that they had full access to all of the data in this study, and the authors take complete responsibility for the integrity of the data and the accuracy of the data analysis.

Declarations

Ethics approval and consent to participate

Ethics approval and consent to participate were taken from our institute ethical committee (Faculty of Medicine—Ain Shams University) with a written informed consent taken from all patients under study.

Consent for publication

All patients included in this research were fully conscious and older than 16 years old and gave written informed consent to publish the data contained within this study. All researchers are accepting to publish this original article in the *Insight into Imaging*. This study is not previously published nor submitted elsewhere, and the methods employed respect the Helsinki Declaration of 1975, as revised in 1983.

Competing interests

The authors declare that they have no competing interests.

Author details

¹Radiology Department, Faculty of Medicine, Ain Shams University, Cairo, Egypt. ²Pediatrics Department, Faculty of Medicine, Ain Shams University, Cairo, Egypt.

Received: 13 April 2022 Accepted: 1 August 2022

Published online: 04 September 2022

References

1. Agha M, Eid AF, Sallam M (2013) Sickle cell anemia: imaging from head to toe. *Egypt J Radiol Nucl Med* 44:547–561
2. El-Hazmi MAF, Al-Hazmi AM, Warsy AS (2011) Sickle cell disease in Middle East Arab countries. *Indian J Med Res* 134(5):597–610
3. Ware RE, Montalembert MD, Tshilolo L, Abboud MR (2017) Sickle cell disease. *Lancet* 390:311–323
4. Clark PR, St Pierre TG (2000) Quantitative mapping of transverse relaxivity (1/T(2)) in hepatic iron overload: a single spin-echo imaging methodology. *Magn Reson Imaging* 18:431–438
5. Fung EB, Harmatz P, Millet M, et al. (2007) Morbidity and mortality in chronically transfused Subjects with thalassemia and sickle cell disease. *Am J Hematol* 82:255–265

6. Wood JC, Ghugre N (2008) MRI assessment of excess iron in thalassemia, sickle cell disease, and other iron overload diseases. *Hemoglobin* 32:85–96
7. He T (2014) Cardiovascular magnetic resonance T2* for tissue iron assessment in the heart. *Quant Imaging Med Surg* 4(5):407–412
8. Restaino G, Meloni A, Positano V, et al. (2011) Regional and global pancreatic T2* MRI for iron overload assessment in a large cohort of healthy subjects: normal values and correlation with age and gender. *Magn Reson Med* 65:764–769
9. Raghupathy R, Manwani D, Little JA (2010) Iron overload in sickle cell disease. *Adv Hematol* 2010:1–9
10. Cramer JA, Roy A, Burrell A, et al. (2008) Medication compliance and persistence: terminology and definitions. *Value Health* 11:44–47
11. Silvilairat S, Sittiwangkul R, Pongprot Y, Charoenkwan P, Phornphutkul C (2008) Tissue Doppler echocardiography reliably reflects severity of iron overload in pediatric patients with beta-thalassemia. *Eur J Echocardiogr* 9:368–372
12. Wood JC (2011) Impact of iron assessment by MRI. *Hematology* 2011:443–450
13. Carpenter JP, He T, Kirk P, et al. (2011) On T2* magnetic resonance and cardiac iron. *Circulation* 123:1519–1528
14. Garbowski MJ, Carpenter JP, Smith G, Pennell DJ, Porter JB (2009) Calibration of improved T2* method for the estimation of liver iron concentration in transfusional iron overload. *Blood* 114:2004
15. Garbowski MW, Carpenter J, Smith G, et al. (2014) Biopsy-based calibration of T2* magnetic resonance for estimation of liver iron concentration and comparison with R2 Ferriscan. *J Cardiovasc Magn Reson* 16(40):1–11
16. Fernandes JL, Sampaio EF, Verissimo M, et al. (2011) Heart and liver T2* assessment for iron overload using different software programs. *Eur Radiol* 21:2503–2510
17. He T, Gatehouse PD, Smith GC, Mohiaddin RH, Pennell DJ, Firmin DN (2008) Myocardial T2* measurements in iron overloaded thalassemia: an in vivo study to investigate optimal methods of quantification. *Magn Reson Med* 60:1082–1089
18. Westphalen ACA, Qayyum A, Yeh BM, et al. (2007) Liver fat: effect of hepatic iron deposition on evaluation with opposed phase MR imaging. *Radiology* 242(2):450–455
19. Queiroz-Andrade M, Blasbalg R, Ortega CD, et al. (2009) MR imaging findings of iron overload. *Radiographics* 29(6):1575–1589
20. Clarke L, Kidson-Gerber G, Moses D, Wu GM-C, Lindeman R (2016) T2* MRI correlates with R2 liver iron concentration in transfusion dependent thalassaemia. *J Hematol Blood Disord* 2(1):1–5
21. Noetzli LJ, Carson SM, Nord AS, Coates TD, Wood JC (2008) Longitudinal analysis of heart and liver iron in thalassemia major. *Blood* 112:2973–2978
22. St Pierre TG, Clark PR, Chua-anusorn W, et al. (2005) Noninvasive measurement and imaging of liver iron concentrations using proton magnetic resonance. *Blood* 105(2):855–861
23. Wood JC (2007) Magnetic resonance imaging measurement of iron overload. *Curr Opin Hematol* 14:183–190
24. Henninger B, Alustiza J, Garbowski M et al (2020) Practical guide to quantification of hepatic iron with MRI. *Eur Radiol* 30:383–393
25. Alexiou E (2014) Methodologies and tools used today for measuring iron load. *Thalassemia Rep* 4(4861):7–11
26. Westwood M, Anderson LJ, Firmin DN, et al. (2003) A single breath-hold multiecho T2* cardiovascular magnetic resonance technique for diagnosis of myocardial iron overload. *J Magn Reson Imaging* 18:33–39
27. Wood JC, Noetzli L (2010) Cardiovascular MRI in thalassemia major. *Ann N Y Acad Sci* 1202:173–179
28. Olivieri NF (2001) Progression of iron overload in sickle cell disease. *Semin Hematol* 38(1 Suppl 1):57–62
29. Musallam KM, Cappellini MD, Wood JC, et al. (2011) Elevated liver iron concentration is a marker of increased morbidity in patients with β thalassemia intermedia. *Haematologica* 96:1605–1612
30. Angelucci E, Muretto P, Nicolucci A, et al. (2002) Effects of iron overload and hepatitis C virus positivity in determining progression of liver fibrosis in thalassemia following bone marrow transplantation. *Blood* 100(1):17–21
31. Fung EB, Harmatz PR, Lee PD, et al. (2006) Increased prevalence of iron-overload associated endocrinopathy in thalassemia versus sickle-cell disease. *Br J Hematol* 135(4):574–582
32. Wood JC, Tyszkla JM, Carson S, Nelson MD, Coates TD (2004) Myocardial iron loading in transfusion-dependent thalassemia and sickle cell disease. *Blood* 103:1934–1936
33. Taghizadeh Sarvestani R, Moradveisi B, Kompany F, Ghaderi E (2016) Correlation between heart and liver iron levels measured by MRI T2* and Serum ferritin in patients with β -thalassemia major. *Int J Pediatr* 4(3):1559–1567
34. Meloni A, Puliyl M, Pepe A, Berdoukas V, Coates TD, Wood JC (2014) Cardiac iron overload in sickle-cell disease. *Am J Hematol* 89:678–683
35. Wood JC, Glynos T, Thompson A, et al. (2011) Relationship between labile plasma iron, liver iron concentration, and cardiac response in a deferasirox monotherapy trial. *Haematologica* 96(7):1055–1058
36. Au W, Lam WW, Chu W, et al. (2008) A T2* magnetic resonance imaging study of pancreatic iron overload in thalassemia major. *Haematologica* 93(1):116–119
37. Karafin MS, Koch KL, Rankin AB, et al. (2015) Erythropoietic drive is the strongest predictor of hepcidin level in adults with sickle cell disease. *Blood Cells Mol Dis* 55(4):304–307
38. Porter JB, Walter PB, Neumayr LD, et al. (2014) Mechanisms of plasma non-transferrin bound iron generation: insights from comparing transfused diamond blackfan anemia with sickle cell and thalassemia patients. *Br J Hematol* 167(5):692–696
39. Walter PB, Fung EB, Killilea DW, et al. (2006) Oxidative stress and inflammation in iron-overloaded patients with beta-thalassemia or sickle cell disease. *Br J Hematol* 135:254–263
40. Vichinsky E, Butensky E, Fung E, et al. (2005) Comparison of organ dysfunction in transfused patients with SCD or beta-thalassemia. *Am J Hematol* 80:70–74
41. Inati A, Musallam KM, Wood JC, Sheikh-Taha M, Daou L, Taher AT (2009) Absence of cardiac siderosis by MRI T2* despite transfusion burden, hepatic, and serum iron overload in Lebanese patients with sickle cell disease. *Eur J Hematol* 83:565–571
42. Noetzli LJ, Coates TD, Wood JC (2010) Pancreatic iron loading in chronically transfused sickle cell disease is lower than in thalassemia major. *Br J Haematol* 152:229–233
43. Yassin M, Soliman A, De Sanctis V, et al. (2017) Liver iron content (LIC) in adults with sickle cell disease (SCD): correlation with serum ferritin and liver enzymes concentrations in transfusion-dependent (TD-SCD) and non-transfusion dependent (NT-SCD) patients. *Mediterr J Hematol Infect Dis* 9(1):1–6
44. Wood JC (2017) The use of MRI to monitor iron overload in SCD. *Blood Cells Mol Dis* 67:1–6
45. Schein A, Enriquez C, Coates TD, Wood JC (2008) Magnetic resonance detection of kidney iron deposition in sickle cell disease: a marker of chronic hemolysis. *J Magn Reson Imaging* 28(3):698–704

Publisher's Note

Springer Nature remains neutral with regard to jurisdictional claims in published maps and institutional affiliations.

Submit your manuscript to a SpringerOpen[®] journal and benefit from:

- Convenient online submission
- Rigorous peer review
- Open access: articles freely available online
- High visibility within the field
- Retaining the copyright to your article

Submit your next manuscript at ► [springeropen.com](https://www.springeropen.com)